We are IntechOpen, the world's leading publisher of Open Access books Built by scientists, for scientists

5,300
Open access books available

130,000
International authors and editors

155M
Downloads

Our authors are among the

154
Countries delivered to

TOP 1%
most cited scientists

12.2%
Contributors from top 500 universities

CLARIVATE ANALYTICS BOOK CITATION INDEX INDEXED

WEB OF SCIENCE™

Selection of our books indexed in the Book Citation Index in Web of Science™ Core Collection (BKCI)

Interested in publishing with us?
Contact book.department@intechopen.com

Numbers displayed above are based on latest data collected.
For more information visit www.intechopen.com

14

Delayed Fracturing: Acoustic Emission Analysis of Nucleation and Transformation of an Ensemble of Mesoscopic Cracks in Deforming Heterogeneous Materials

Albert Leksovskii
Ioffe Physical – Technical Institute, Russian Academy of Sciences, St. Petersburg, Russia

1. Introduction

Acoustic emission is accompanied by many physical processes and phenomena, including discrete structural changes in solids during deformation. Information about these processes is very important for determination of the resource strength and durability of elements of machines and constructions in order to monitor and prevent technogenic catastrophes. Submitted experimental results demonstrate the unique capabilities of acoustic emission method in the analysis of nucleation and transformation of an ensemble of micro- and mesocracks. This allows us to formulate adequate, physically based models of the process of material damage in the course of its operation.

A lot of conventional engineering materials, such as polymers, metals, composites, as well as coarsely heterogeneous materials (rocks, concrete etc.), response on the applied deformation through the nucleation of microscopic and mesoscopic cracks. Such cracks could appear in a short time after the load application, and so cracked material might work a long time. Under condition of long-term operation under loading, these cracks in many cases allow one to use a concept of damaging that is deterioration of physical and mechanical properties. There is very limited information on the nucleation and transformation of the crack ensemble up to now. How far and under which conditions do cracks of micro- and mesoscopic size determine altogether the performance of material and the critical state of loaded body? Our study is to elucidate the real properties of both individual mesocracks and the ensemble of such cracks.

The cracks of micro- and meso-scale play, far and away, the role of indicators of local critical state of structure. These defects, which, undoubtedly, accumulate in a solid under the action of mechanical stress, are regarded as damages. A lot of microscopic studies of metals evidence (Botvina, 2008, among many others) that cracks of meso-scale are presented in multitude in vicinity of stress concentrators, in localities of heterogeneous development of inelastic deformation. And the ensembles of such cracks, what is their role? The ensemble/cluster of cracks is an entity that gives rise to the probability of the

direct elastic interaction between defects in heterogeneous materials that exhibit microplasticity. Is this an unavoidable formation that specifies a necessary stage of the main crack nucleation? Does one might regard such the ensemble as an idiosyncratic embryo of the main crack? Or else any other physical mechanism underlies the organization of the critical state of deformable solid?

The diffraction techniques (Regel', Slutsker & Tomashevskii, 1974, Kraus at al., 1993, Schors at al., 2006,) give precious few information on the nucleation and development of the microcrack ensemble with the exception of the fact that these ensembles are formed quite rapidly (say, in creep mode), and then their further evolution becomes, really, exhausted. As a rule, it is postulated that even the cracks of such a scale can be regarded a priori as conventional stress concentrators (Arias et al., 2003, Bouchbinder at al., 2004, Nasseri at al., 2006 among others); to our best knowledge, the latter postulate was not confirmed experimentally.

Moreover, this approach was not justified in SEM in situ experiments (Leksowskij & Baskin, 2011). Contrariwise, the ensemble of a limited number of microcracks appearing in a short time interval at a certain stage of the microcrack growth inhibits the steady crack propagation.

As regards conventional engineering materials, there are no any appropriate instrumental opportunities to monitor in real time not only the interactions between micro- and meso-cracks but also the evolution of the crack ensemble as a whole.

However, one could expect that the application of amplitude-time statistical analysis of acoustic emission (AE) signals in a mode of linear location might substantially extend our conceptualization of multiple-site microdamaging in deforming heterogeneous materials with uniform structure. A great difference in physical and mechanical properties between the host material and reinforcing fibers ensures preferred breaking of high-modulus elements under conditions of common deforming, thus providing the unambiguous identification of the AE source from measurements of signal amplitudes. In the case of composites, one can establish the structure, vary the properties of elements, control the nucleation of the collection of cracks of the given size, investigate some statistical aspects of nucleation and development of the ensemble of such cracks; using a linear location method, even the nucleation and evolution of a particular, limited group of cracks could be traced both in time and in the given sample cross-section. In addition, one could consider not only the behavior of a model sample but also a response of the real engineering material with the same structural elements.

2. Samples and equipment

The samples for a SEM in situ study were made of hot solidified epoxy resin and shaped to a double trowel with the working part of 10×6×(0.7-1) mm, and they had artificial stress concentrator (incision). In order to eliminate the surface charge, the samples were preliminary saturated by iodine. Finally, they were dark-cherry-coloured, quite brittle; their ultimate strength was about 25-35 MPa. The samples' geometry and the thermal treatment provided the stressed state close to that of plain strain type.

The composites based on either carbon or boron fibers of 7-8 μm and 100 μm in diameter, respectively, were used for an AE study. The selected composites differed in the scale of structural elements and, correspondingly, in the size of defects generated under stretching.

Let us consider consistently how the AE technique allows one to obtain direct information on the nucleation of defects of the scale of structural elements, on ensemble of such defects, on cooperative effects in behavior of defects under conditions of active stretching of special model samples as well as samples of real composite materials.

The main equipment set for carrying out the AE study was developed at the Kurchatov Atomic Energy Institute. The analogue module provided the processing speed not less than 10^3 pulse/s, so, the time interval τ between resolved pulses in train was not shorter than 1 ms. The dynamic amplitude range was not less than 60 dB; the operating frequency band was 0.1-1.1 MHz with nonuniformity of amplitude frequency response ± 3 dB; the noise level as reduced to preamplifier input was not more than 3 μV. The output of digital block included the following data: signal amplitude A (μV), number of oscillations (i. e. number of excesses of discrimination threshold), signals/events duration θ (ms), intensity $\dot{N}$ (number of AE signals/events per time unit, N/s), signal energy ($W = V^2\theta$), signal power $\acute{W}$ ($V^2 \times \theta$/s), energy per pulse (W/pulse); time difference between signals detected by antenna transducers (for determination of coordinates of signal source). In the case of 3D presentation, the knowledge of the latter parameter enhances substantially the information content and reduces a field of hypothetical speculations.

The samples were model materials composed of polymer and metal matrices reinforced by uniaxially oriented carbon or boron fibers. In the case of epoxy-based CFRP (binders ED-20, EDT-1, and EFNB; carbon strip ELUR-P 0.1), the samples were shaped to plates of 160×(7-10)×(0.3-1) mm. The volume content of fibers with diameter of ~7-8 μm was $V_f \approx 60\%$.

The boron-aluminium samples D16T-B were prepared by diffused pressure welding. The size of the test section was 2.1 × 4.3 × 22 mm; the volume content of fibers with diameter of 100 μm was 1, 2.5, and 18 %. There were approximately 30 fibers in the cross-section of the sample D16 –B (2.5%). Samples of the composite based on the aluminium alloy AMG61 were prepared by plasma-sputtering technique; boron fiber content was 43 %. The deformation rates were 0.017, 0.118, or 0.525 mm/min at 20, 200, or 300^0 C. Two piezoceramic transducers with resonance frequency of 400±50 kHz were fixed on the test section at the distance of 80-100 mm one from another.

3. SEM in situ experiment

Let us consider briefly some previously unknown features related with the nucleation and evolution of individual microcracks .

Certain aspects of the nucleation and development of micro- and mesocracks are available from in situ studies of model samples made of conventionally “structure-free” polymer with the help of the SEM technique.

The experiments have shown the following: i) microcracks nucleate in an explosive fashion, and then their initial velocity of propagation decreases in approximately two orders of magnitude (fig. 1a); and ii) the crack nucleation is the event with the inevitable relaxation of the finite-amount, elastically accumulated energy (fig. 1b).

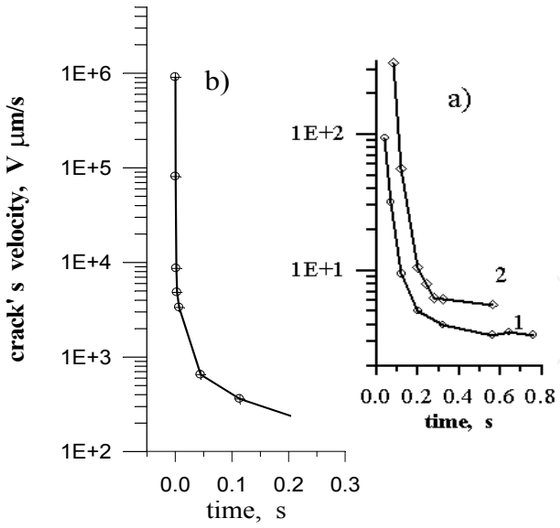

Fig. 1. Instant rate variation of newly nucleated "natural" microcrack *a)* at the initial (*1*, l_0 = 0.5 μm) and final (*2*, l_0= 0.9 μm) stages of crack formation, and *b*) in the case of crack initiating in the bulk polymer due to a rupture of high-modulus d = 100 μm boron fiber.

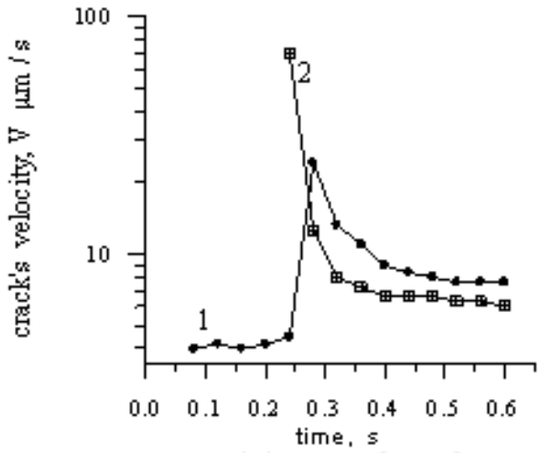

Fig. 2. Variation of the propagation velocity of an "old" crack (1) of 5 μ in length caused by the nucleation of a new crack (2) of 1.5 μ in length in its neighborhood.

The experiment has shown (see fig. 2) that the strain energy that releases due to the generation of microcracks in the course of the relaxation-evoked redistribution exerts the short-term (but considerable) change of the velocity of neighbouring "old" microcrack. It was found also that the final size of a (micro-) mesocrack depends on the dissipative properties of material (see fig. 3).

From the data presented in fig. 4, one can conclude that the dissipative properties of material influence the crack propagation rate and on the rate of local stress redistribution. The distribution maximum is not at all in the time interval of elastic interactions (1–3 μs) but falls in the range of 10^2 μs or even 10^3 μs in dependence of the dissipative properties of the matrix. Thus, one can state that the dissipative properties of the matrix could play the role of a regulator of stress redistribution (Tishkin, Gubanova, Leksowski & Yudin, 1994)

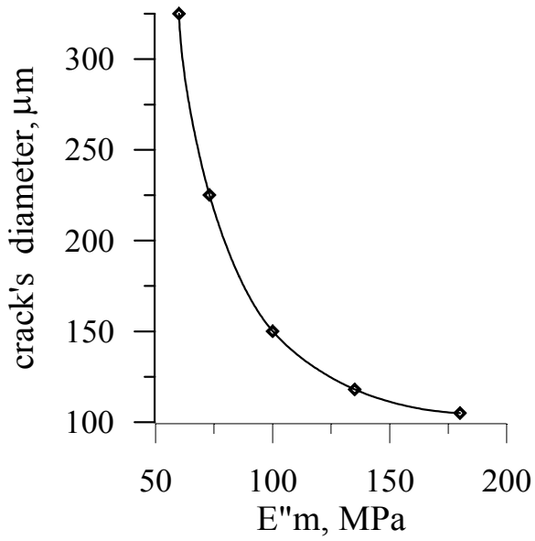

Fig. 3. Dependence of the critical diameter d_{cr} of crack in the model composite on the maximum modulus of mechanical losses E''_m of the Rolivsan binder used as a matrix.

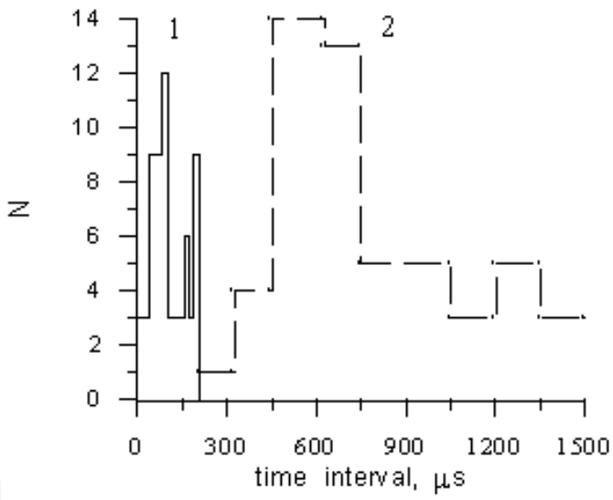

Fig. 4. Histograms of the numeric distribution of time intervals between acoustic emission signals for the carbon plastics based on (1) PEI-N and (2) PEI matrix.

The data shown in fig. 4 demonstrate that the breakage of neighboring fibers in real carbon fiber reinforced plastics, CFRP, (V_f ~ 60% carbon fibers) may occur in the course of the relaxation redistribution of local stresses [4]. In this case, the time interval between neighboring breaks ranges from tens of microseconds to hundreds of milliseconds. These times are much longer than the time of the redistribution of the elastic stress (for the given CFRP structure, the temporal range of elastic interaction is 1-3 μs) but they are sufficiently short to neglect any increase of the external stress in these experiments. In other words, the dissipative properties of materials affect the rate of the stress relaxation redistribution, thus delaying a break of neighboring fiber after the primary fiber rupture. This evidences directly the prevailing role of the relaxation mechanism of local stress redistribution in the competition of elastic mechanism in microdamaging.

The in situ SEM data and model experiment confirmed the fact of the presence of both the dynamic and relaxation stages in development of newly-born (micro-) mesocracks. It is very important to note, that the explosion-like formation of a microcrack is related to a discrete change in the local strain energy with the inevitable subsequent transient relaxation process.

4. Ensemble of cracks of the scale of structural element

4.1 Cracks of 10 μm

Figure 5 shows a fragment of the load-extension diagram for the special model ED-20-based sample with a single fiber, and results of AE signals detection under stretching with the rate of 0.017 mm/min. As the fiber reaches its ultimate strain (~1.1 %), its fragmentation begins. Number of detected AE pulses and coordinates of failures calculated from the location data coincide quite well with the same data on number of failures and coordinates found in direct microscopic measurements. 50-60 failures were detected along the test section length of 40 mm. The statistical processing of lengths of broken fibers in a series of identical samples gives the estimated average value equal to ~ 280 μm.

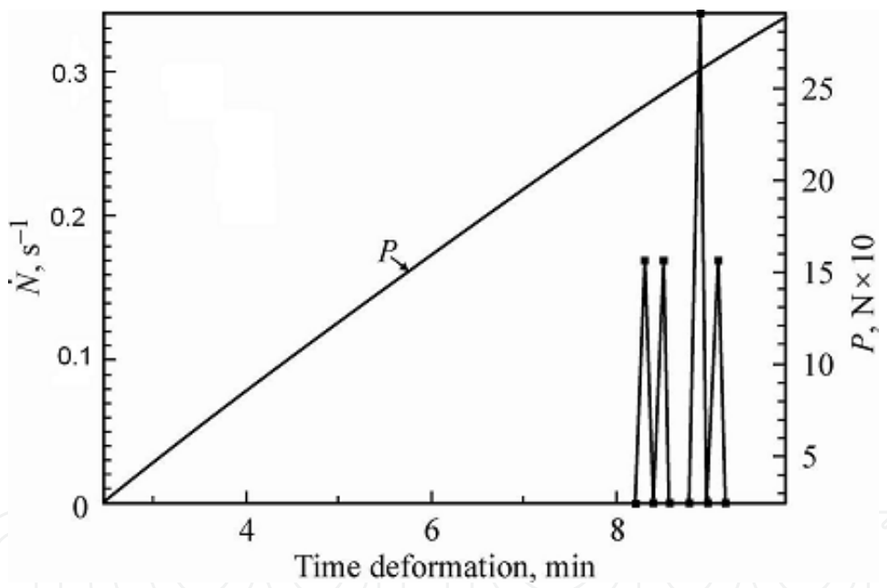

Fig. 5. Variation of AE intensity Ṅ from loaded sample containing a single fiber.

The amplitude distribution of AE signals is depicted in fig. 6. The value of the AE signal amplitude from a single failure (as reduced to input of preamplifier) was 90-130 μV. It should be noted that the observed dispersion of signal amplitudes could be due to a number of causes, such as variation of sample strength along its length, signal decaying, and inaccuracy of fiber positioning in the sample relatively the axis of loading. The latter inaccuracy results in emerging of a shear component and, correspondingly, reduces the value of ultimate stress. The average amplitude value, Ā, which is equal to ~ 100 μV, could be regarded as first approximation when estimating the number of simultaneously (here within 1 ms) broken fibers.

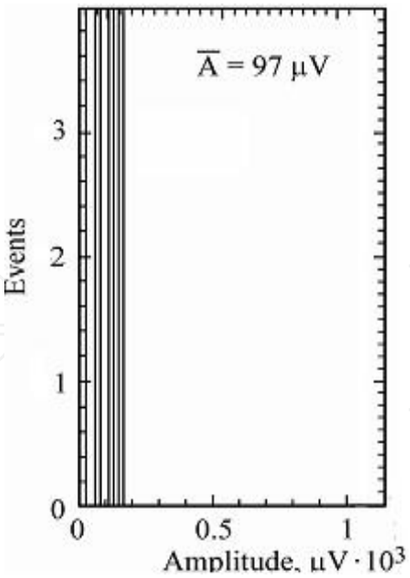

Fig. 6. Amplitude distribution of AE signals.

Now we shall consider the behavior of uniaxially reinforced sample that contained not one but a few thousands of carbon fibers, the volume content of which, V_f, was about 60 %. A fragment of the microscopic structure of pressed plastics is depicted in fig. 7.

We shall consider how the accumulation of fiber failures, that is crack-like damages, occurs in the sample stretched along the direction of reinforcing. What happens in heterogeneous system when in spite of a single crack comparable in size with structural elements, a certain multitude of cracks appears?

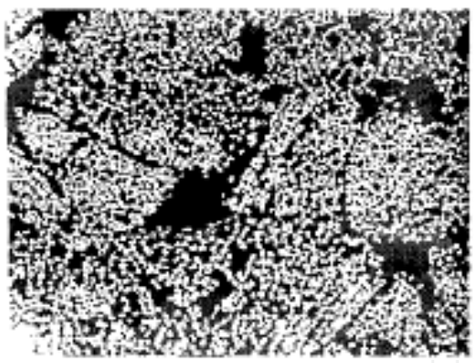

Fig. 7. A fragment of the cross-sectional sample CFRP

The location of AE signals (see Fig. 8) demonstrates that the process of fiber failures under constant rate deformation flow neither gradually nor avalanche-like but consists of alternate stages of acceleration and deceleration. A break of the sample occurred in the region with coordinate (5-13) mm. One can see that this locality did not exhibit any particularities during all the deformation cycle. There were neither multiple failures of fibers nor any other signs of "preliminary preparation" of the macroscopic failure. The fiber breakage process in adjacent zones is well pronounced at particular stages of deforming. The intensive process of fiber breakage was observed at coordinates (21-13) mm in the time interval 1 to 5 minutes.

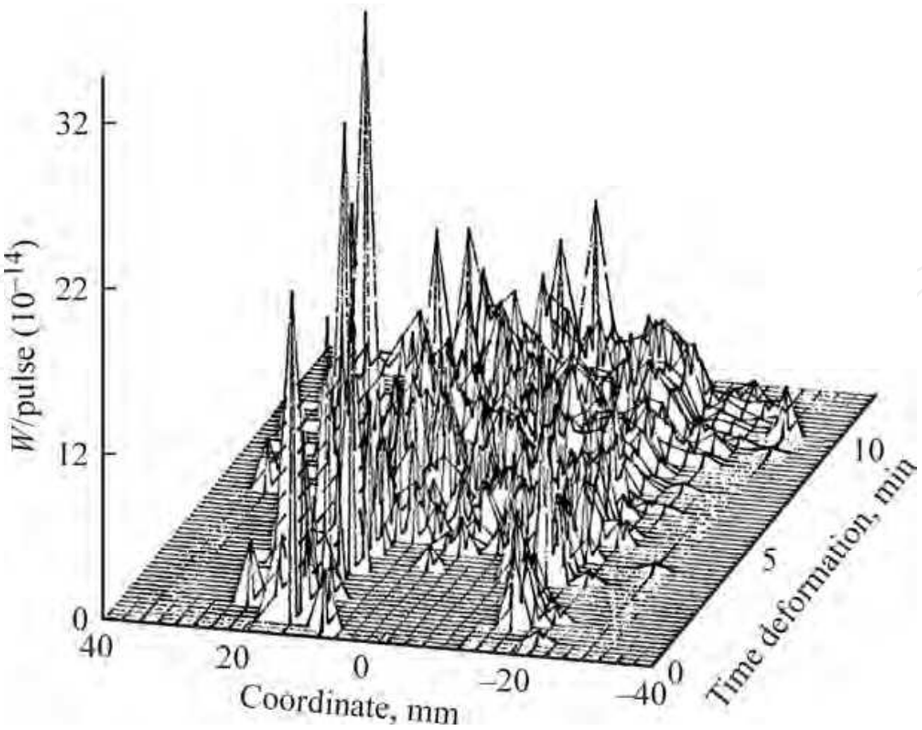

Fig. 8. Variation of average energy in pulse (AE event) over cross-section of CFRP with fiber content of 60 % as deformation increases. The deformation rate 0.22 mm/min.

Nevertheless, there was not a further process localization in this particular volume. The appearance of a group of cracks could reduce the effective elastic module of this part of the sample with inducing the load redistribution. It will be seen below that the locality and time of macroscopic damage are not due to previous damaging of any domain but caused by the dynamics of the energy dissipation processes, which leads to the exhausting of the energy capacity of system.

Let us consider this process in details with the help of the statistical analysis of trains of AE signals from different sites.

On should expect the existence of the interrelation between AE events because the AE source is related, predominantly, with the crack nucleation. According to the data of in situ SEM experiment (Leksowskij & Baskin, 2011), a microscopic crack cannot nucleate without leaving a trace in its nearest environment; such an event is accompanied by either a short-term acceleration of neighboring crack or a nucleation of the new one.

The using of equipment which provides the precise determination of pulse arrival allows one to perform the AE time analysis by constructing the function of distribution of time intervals between pulses. To obtain correct data from the statistical analysis, one should provide sufficiently representative sampling (70-100 signals); in addition, the process itself should be essentially stationary. For example, the intensity variation in the train of AE pulses, as a rule, should not exceed 20 %. In the case of complete independence of AE signals, the process is regarded as poissonian with the following analytical representation $\rho(\Delta\tau) = m \times \exp(-m\Delta\tau)$, where m is the event frequency, $m = \dot{N}$ (AE intensity); $\Delta\tau$ is the time interval between events; $\rho(\Delta\tau)$ is the probability density.

Now we shall consider the distribution of time intervals between AE pulses in certain sample cross-sections and in different instances of deformation in order to reveal some particular features that would evidence the presence of correlation and interrelation between failures of reinforcing fibers. Figure 9a shows an example of Poisson distribution of time intervals between AE pulses from a deforming CFRP detected at the time interval (480-510) s in zone (5-13) mm taken from the whole diagram W/pulse (l, t) (fig. 8).

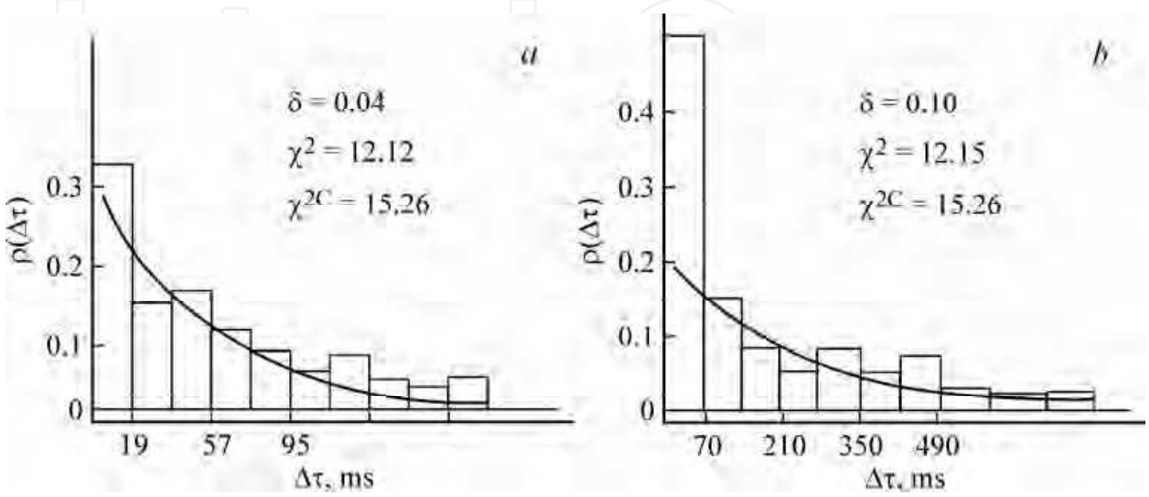

Fig. 9. Distribution of time intervals between pulses in zone of future failure at different stages of deforming.

One can see that in this case the distribution of time intervals between pulses does not differ from the theoretical (poissonian) exponential distribution. This means that the fiber failures process in this locality is independent, poissonian process. However one could expect that such a situation takes place not always and not in any place. Figure 9b shows the distribution of time intervals between pulses in the same part of the whole diagram (5-13) mm but at the later stage of deforming (590-616) s. This distribution differs from the theoretical (poissonian) one. The main deviation is observed in the time interval ~ 70 ms. In such a case, one may suggest the poissonian process of crack accumulation (Tishkin and Leksowski, 1988) with a certain local ordering though the events in complete flow remain independent. The parameter $\delta = | 1 - \bar{\Delta\tau} / \sigma_{\Delta\tau} |$ may serve as a quantitative measure of such ordering (deviation from poissonian-like process) (Braginski, Vinogradov and Leksowskii , 1986). Here $\bar{\Delta\tau}$ is the average time interval between pulses in the given sampling, and $\sigma_{\Delta\tau}$ is the mean-square deviation. It was revealed that such analysis allows one to obtain more detailed information on the evolving fracture process. Figure 10 shows a variation of the above defined parameter of ordering δ that characterizes the correlation between AE events in deforming CFRP in zone of future failure as well as in two neighboring zones (AE diagram in fig. 8).

One can see in fig. 10 that in the last ~ 30% of the total time of deforming of CFRP sample, the process of fiber failure / crack nucleation begins to pass from the stage of independent, non-connected events to the stage of correlated interactions. This process is more pronounced in localities situated in the vicinity of the zone of future macroscopic failure. Nevertheless, the value of the parameter δ is stable in the future-failure-zone (5-13 mm), and

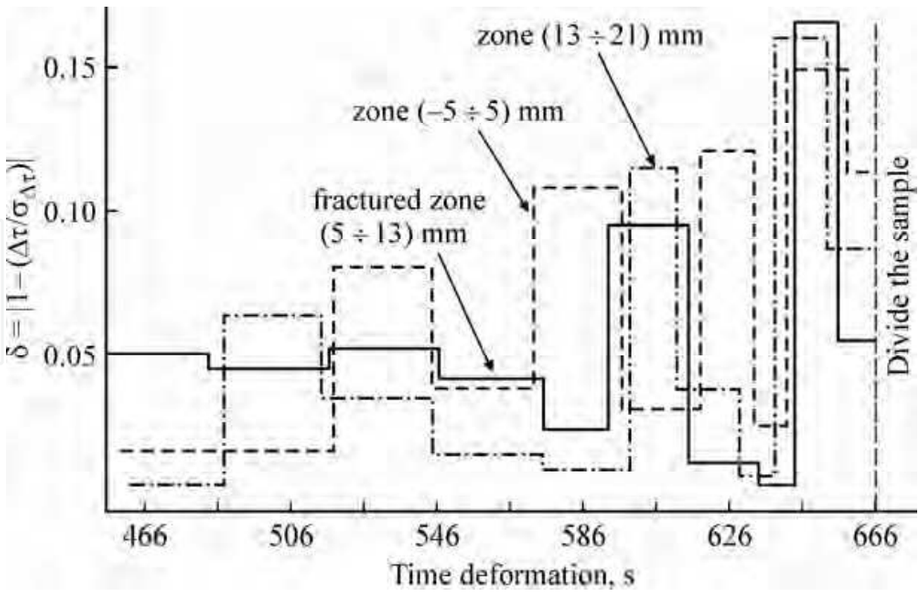

Fig. 10. Variation of the degree of ordering (δ) in the train of AE events from three neighboring local volumes in one-directional CFRP at the deformation rate equal to 0.22 mm/min.

a steady trend of its multi-fold increase is observed. So, there is a growth of ordering and correlation in the train of AE events: each event affects virtually the future ones. This trend is not monotonic but exhibits the pulsating character with periods of decay and growth of tens seconds' length. A certain phase opposition was observed in variations of the degree of ordering in AE trains from local zones in the vicinity of the position of macroscopic damage. The increase of the degree of correlation of AE events (fiber failures /crack nucleation) in a particular zone was accompanied with the deceleration of the fracture process in an adjacent zone characterized by a relative stagnancy. At the same time, it is worthy to note that even a simple conservation of a certain level of correlation in the train of AE signals during a few tens seconds under conditions of the external load increase evidences the effective discharge of the elastic energy concentration in a local volume. It is the reduction of the level of local stresses resulted from intensive structural reconfigurations that suppresses the driving force of local fracture process with exciting it in neighboring sites. Every increase of the value of the parameter δ means the increase of either the total "length" or the number of correlated fiber failures. This is a kind of start of the avalanche-like process that, as one could expect, must result in macroscopic failure. However, every time it turns out to be a false start. One should pay attention to some fine details of the formation of the pre-starting, critical state of deforming sample. In the time interval 630 to 645 s, one can see an additional decrease of the parameter δ in the zone of future failure; simultaneously, the degree of correlation rises sharply in adjacent zones. One more feature: there was a significant drop of the correlation in all three zones during last ten seconds of the deformation cycle. This means that the stress redistribution over neighboring zones takes place in this time interval.

One can see in fig. 11 that the length of trains of correlated crack formation (fiber failures) in the zone of macroscopic failure (5-13) mm at the final stage of deforming (510-660) s is equal to 50-60 μm (2-3 structural elements). There were strong detected signals neither in zone of

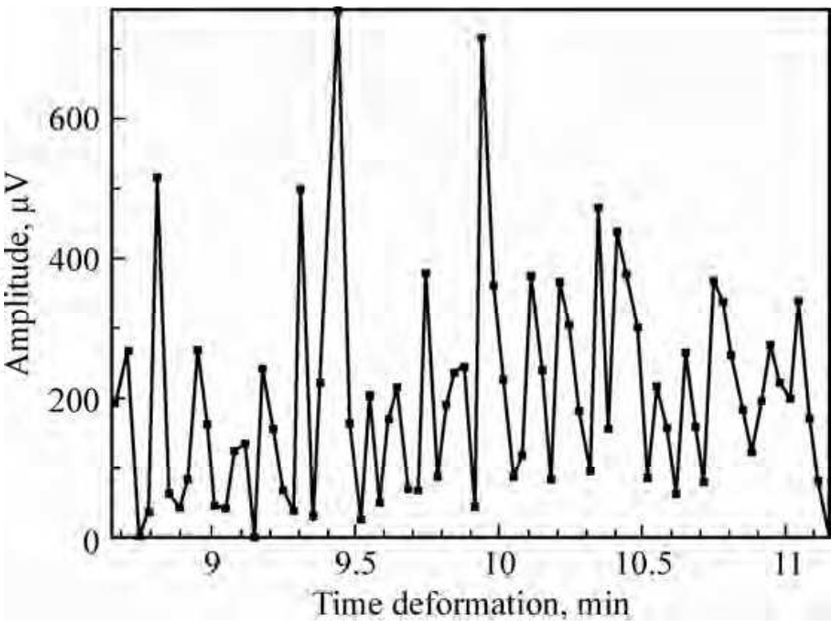

Fig. 11. Variation of AE amplitudes in zone of macroscopic failure during last 150 seconds of deforming of unidirectional carbonplastic.

macroscopic failure, nor in adjacent or any other zones in the last instance (1 ms). The data acquisition system was capable to detect amplitudes that exceed the maximum signals shown in fig. 11 in two orders of magnitude. The actual start of macroscopic failure is, really, out of the sensitivity of this equipment.

So, the statistical analysis of the train of AE signals from deforming composite with small-scale structural elements (7-9 μm) performed in the mode of linear location demonstrated the following:

- the increase of the degree of correlation of AE events (fiber failures / cracking) in a particular sample domain is accompanied with the deceleration of this process in neighboring zones;
- this evidences the effective discharge of concentration of elastic energy in a local volume under conditions of growing external load;
- it is the decrease of the level of local stress resulted from the intensive process of microstructural reconfigurations that suppresses the driving force of this process for a certain time thus inducing the similar process in adjacent domains;
- the existence of ensemble of correlated cracks is neither necessary nor sufficient condition for the formation of main crack.

4.2 Cracks of 100 μm

We shall consider this problem by the example of the composite made of aluminum alloy reinforced by high-modulus, high-strength fibers with the strength distribution shown in fig. 12. Fiber diameter was equal to 100 μm; at large volume content of fibers ($V_f > 30\%$) this composite is very sensitive to neighboring failures. In the case of small volume content, the multiple crashing of fibers takes place, what, as is known, produces in matrix a limited

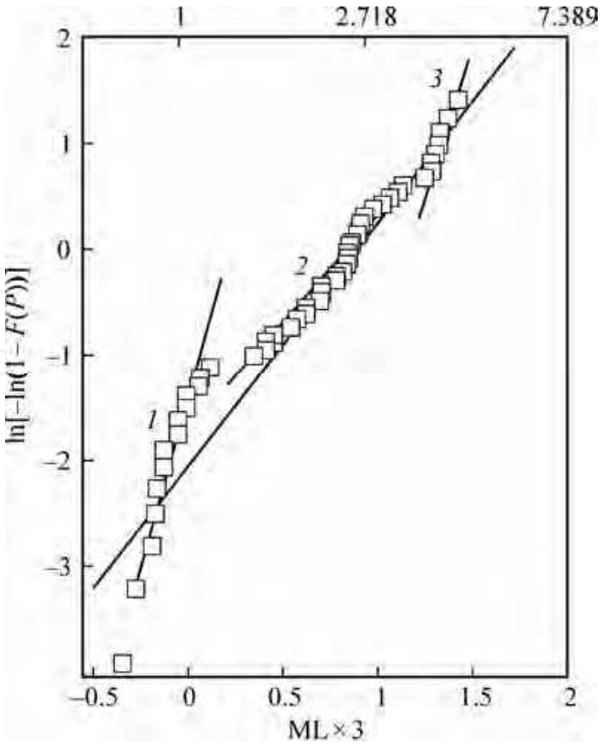

Fig. 12. Weibull distribution of boron fiber strengths

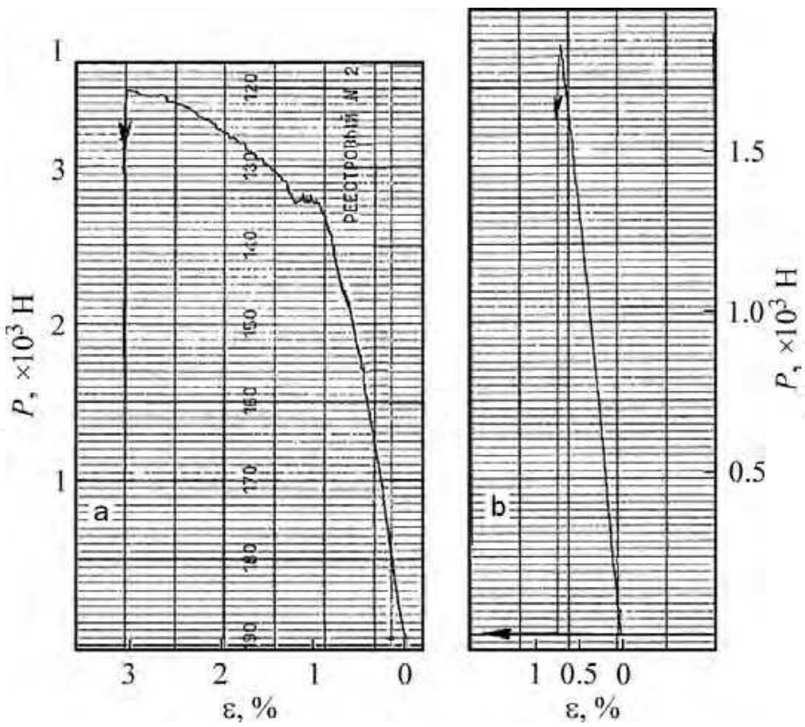

Fig. 13. Load extension curve of samples D16T–B (2.5%) (a) and D16T–B (18%) (b); deformation rate was 0.017 mm/min.

number of cracks at the initial stage of stretching but does not affect the further course of the deformation curve (fig. 13). The dimensions of defects of continuity in the low-modulus host, which appear due to failures of high-modulus fibers, are, unambiguously, close to that of structural elements. Their behavior might be monitored reliably by the method of AE signal location, which allows one to trace the course of events in real time scale. A great part of experiments was carried out with samples containing small amount of reinforcing fibers (V_f = 1 – 2.5%); in this case, the main load was carried by matrix.

The AE signals related to fiber failure are well discriminated from signals from other sources by their amplitude (fig.14), therefore, it will be implied below (unless otherwise specified) that the necessary selection was performed, and the analyzed AE is caused exclusively by fiber failures.

According to the data of metallographic analysis (fig. 15), multiple fiber failures occur in the interval 4000 to 6000 s; then the mayor load is carried by the matrix. A total of fiber failures ranges from 600 to 800.

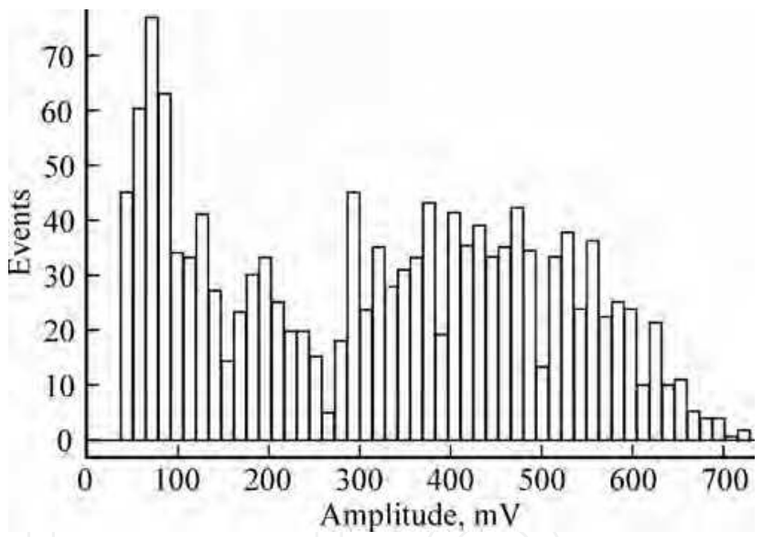

Fig. 14. AE signal amplitude distribution in deforming composite D16T – B(2.5%)

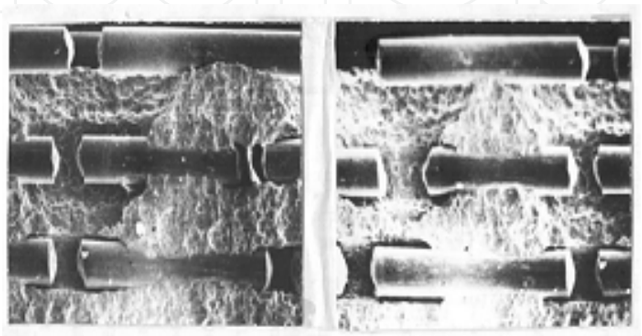

Fig. 15. Fragments of etched sample surface after extension.

Figure 16a shows a plot of the AE activity Ṅ (number of signals per unit of time) over all time of deformation at deformation rate 0.017 mm/min. The final distribution of failures along the sample length, as revealed from the location data (fig. 17), is sufficiently uniform, therefore, the critical fiber length, $1_{cr,}$ might be about 1 mm in agreement with the metallography (fig. 15). The performed analysis showed that independently of the used deformation rate, the region of multiple failures is related with the variation of deformation of ~ 2.5%.

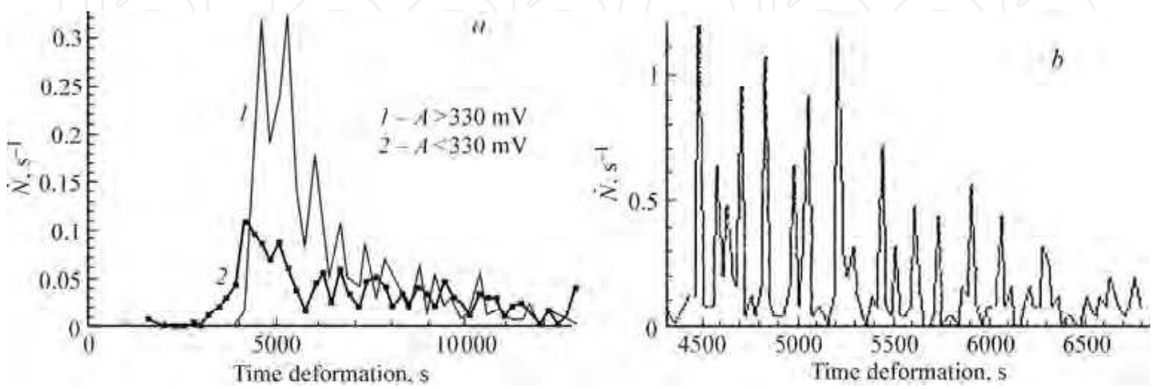

Fig. 16. AE activity (Ṅ, s^{-1}) at deformation rate 0.017 mm/min; (a) shows total time output, (b) shows output in the interval of multiple failures.

The yield of the AE activity in the region of multiple crashing is depicted in fig. 16b in the extended time scale. One can see that in all cases the "fine structure" of the peak of activity manifests itself in splitting of the peak into 12-15 narrow features. The number of signals in these features varies anywhere from 25 to100 % of the total number of fibers in the sample cross-section. The location data confirm the localization of failures in limits of the peak Ṅ in a single section of 2-3 mm. As recalculated into the value of deformation, the distance between the peaks does not depend also on the deformation rate and is equal to 0.1-0.2 % all the time.

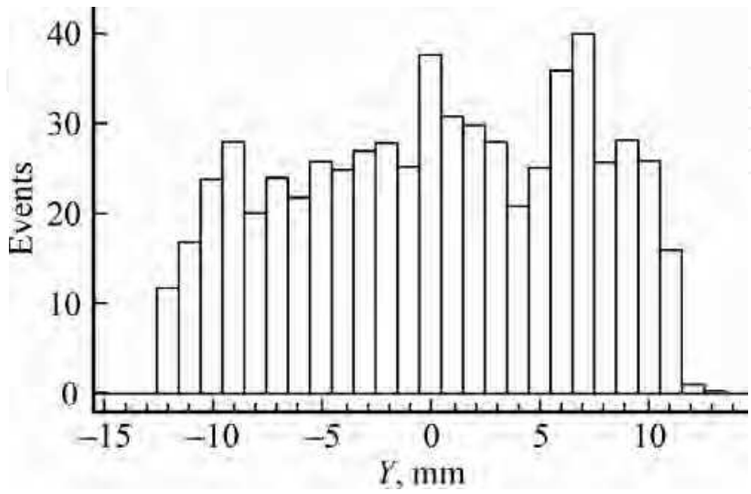

Fig. 17. Final distribution of broken boron fibers along the sample length.

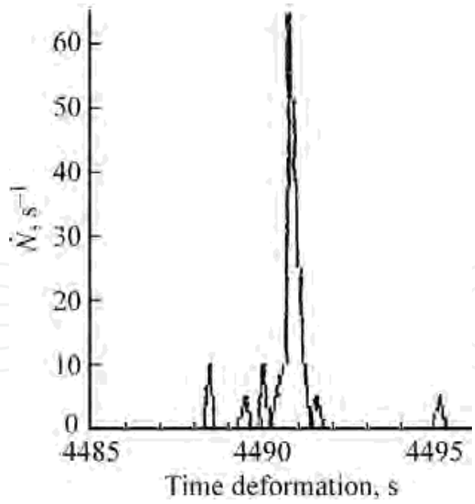

Fig. 18. AE activity in the time interval 4485 to 4495 seconds (see also fig. 16b)

The widths of the peaks themselves (see fig. 18) change approximately 8 times when the deformation rate varies 40 times. In our opinion, this gives one a reason to regard the peak width as invariant not only in the scale of deformation but also in the scale of time. This means that the multiple fiber failure in a single cross-section can be regarded as the process occurring at constant stress and constant strain, that is as the correlated process (Leksowskij at al., 2008). At the same time, it is clear that this process cannot be determined only by the elastic stress redistribution since in this case it would be over in a few microseconds and manifest itself as a very high amplitude signal. Under the given specific conditions, the used equipment would detect the AE signal train consisting of signals separated by intervals shorter than 1 ms as a single signal. As far as in our case the intervals between signals were much longer, one should conclude that the process of correlated fiber failures in the sample cross-section is determined by the relaxation properties of matrix.

Now we shall consider the process of failure of boron fibers / crack formation in this model composite sample in the 3D representation (see fig. 19).

One can see that the process of correlated fiber failures starts in one of the cross-sections in accordance with the Weibull distribution of fiber strengths. However, this process under the given conditions of experiment (deformation rate, temperature) does not cover all fibers in the given cross-section and, all the more so, does not lead to sample failure in this particular place but induces the development of the similar process in the neighboring cross-section. The coordinates of the active cross-section change in one way mode successively and continually with the accuracy limited by 1_{cr}, therefore, the process of fiber failures returns to the initially most active cross-sections. It seems that such a behavior is caused by the fact that the accumulation of failures (mesodefects of continuity) leads to the decrease of the local effective elasticity modulus.

We have seen (fig. 1-2) that the crack nucleation represents an explosive-like event with the inevitable relaxation of the finite-amount, elastically accumulated energy, and that the dissipative properties of material affect the crack size and the rate of local stress redistribution. In the case of suppressed or insufficient dissipative properties (Leksowskij &

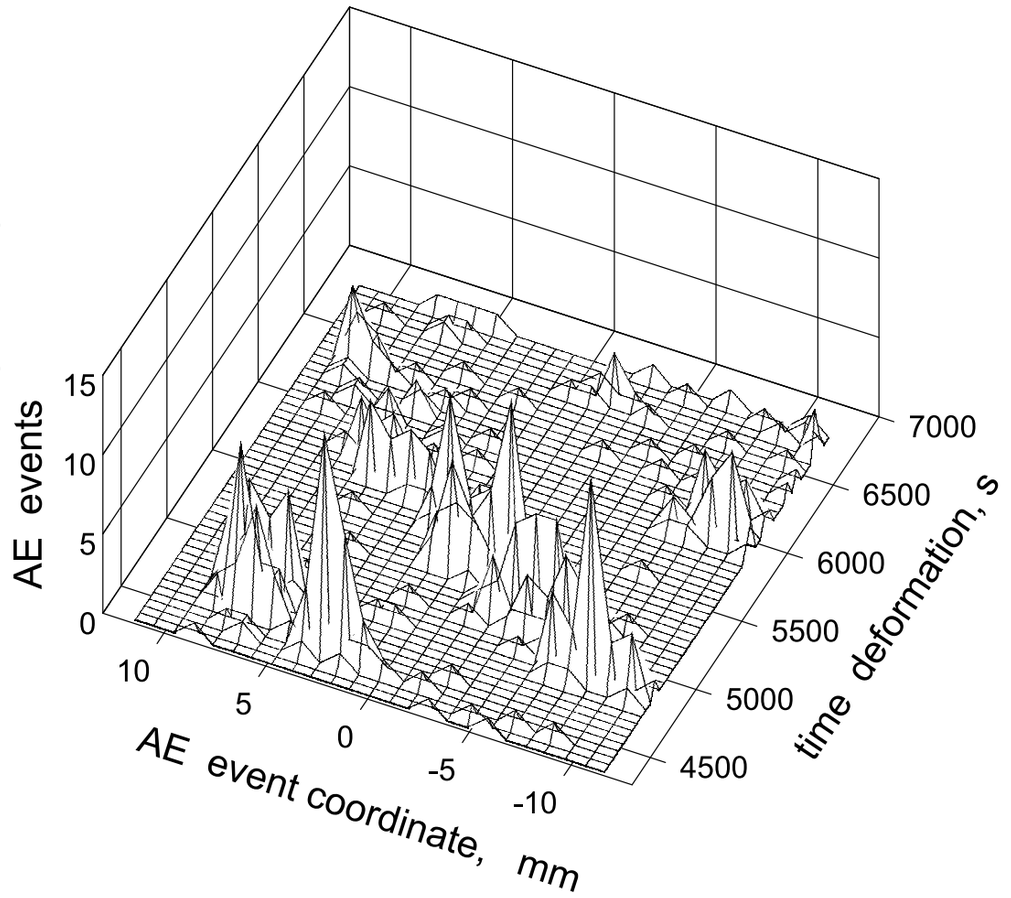

Fig. 19. 3D AE diagram of the fiber failure distribution in the course of sample deforming.

Baskin, 2011), the elastic, linear interaction between defects takes place, and the macroscopic fracture occurs. Therefore, one can control the cracking either through suppressing, minimizing the relaxation component of the local stress redistribution or by gaining the dissipative properties. We shall demonstrate below that in the general case one should consider the dissipative properties of both the nearest environment and the solid as a whole.

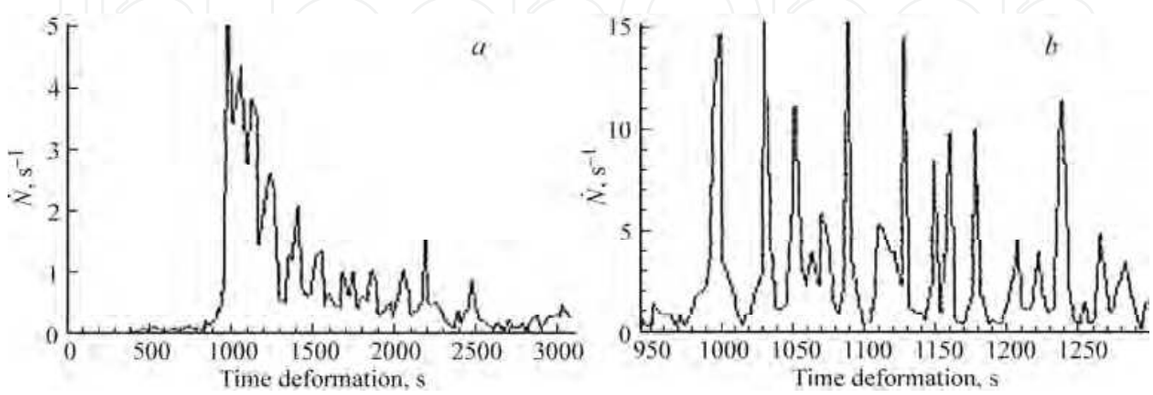

Fig. 20. AE activity Ṅ over all time of deformation of sample D16T – B(1 %) at deformation rate 0.118 mm/min (a), and the same in the time interval of multiple crashing (950 to 1300 s) (b).

When comparing the data presented in fig. 16 and fig. 20, one can see that the increase of the deformation rate a few times (from 0.017 to 0.118 mm/min) resulted in the noticeable increase of crack formation. Consequently, the restriction of the realization of the dissipative properties of matrix leads to the increase of correlated fiber failures per unit of time of deforming.

Figure 21 shows the 3D AE diagram for this sample. In this case, the crashing process started in a certain cross-section and then progressed simultaneously and successively in two different directions.

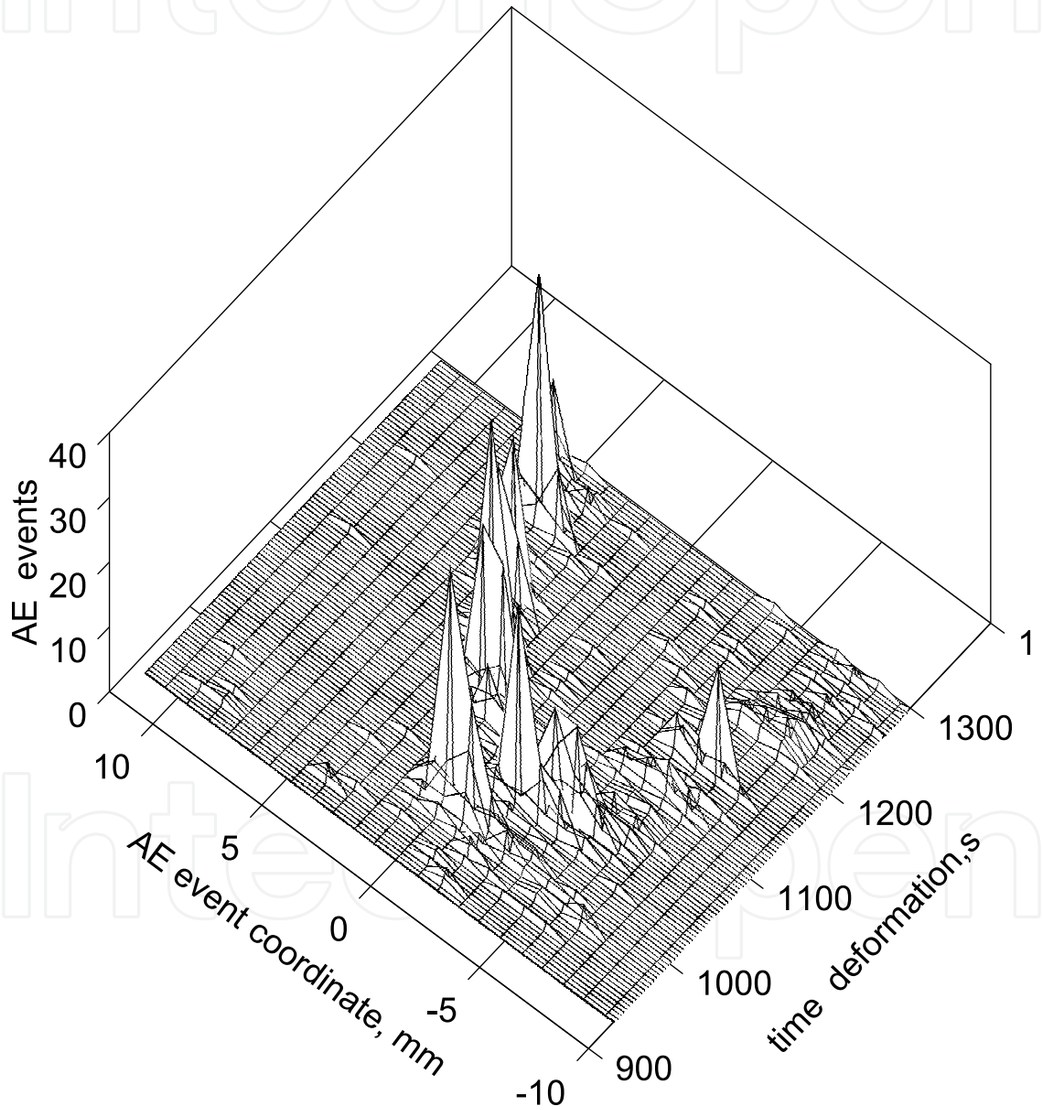

Fig. 21. 3D AE diagram of the fiber failure distribution in the course of deforming of sample D16T – B(1 %) at deformation rate 0.118 mm/min

As the deformation rate increased to 0.545 mm/min (see. fig.22), the process of fiber failures /cracking advanced still faster.

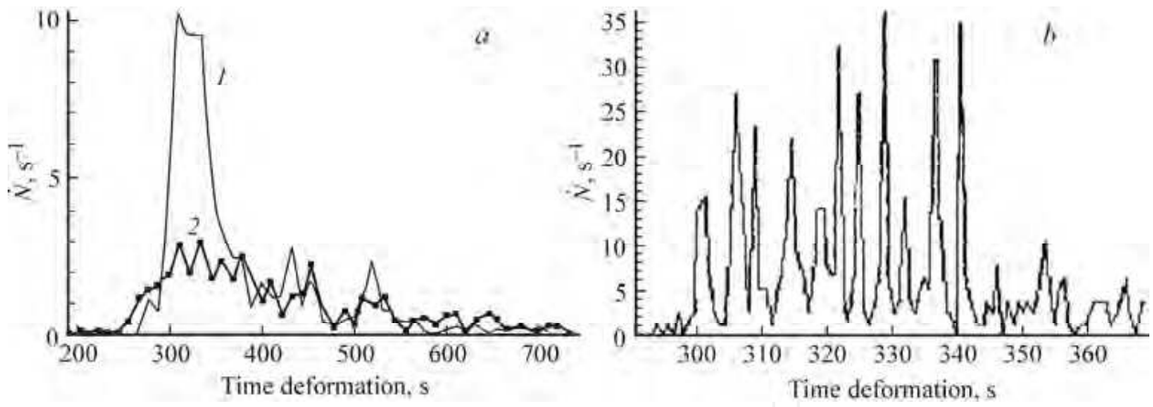

Fig. 22. AE activity Ṅ over all time of deformation of sample D16T – B(2.5%) at deformation rate 0.545 mm/min (a), and the same in the time interval of multiple failures (300 to 370 s) (b). *1* – amplitude AE signals > 270 mV, *2* - amplitude AE signals < 270 mV .

One can see in fig. 23 that at elevated testing temperature (300° C) the process of correlated fiber failure fairly degenerates. Whilst at 20° C and at the same deformation rate of 0.118 mm/min one could see 9-10 bursts of correlated fiber failures, at 300° C, the number of such clusters reduced to 2-3, and the number of fiber failures in each cluster decreased markedly. The 3D AE diagram for this sample as deformed at 300° C is depicted in fig. 24, in which one can see clearly the mentioned particularities. Under conditions providing a more efficient realization of the dissipative properties of matrix in relation to the redistribution of local stresses, the probability of correlated failures is ultimately minimized, and discrete, isolated damages are prevailing in the sample.

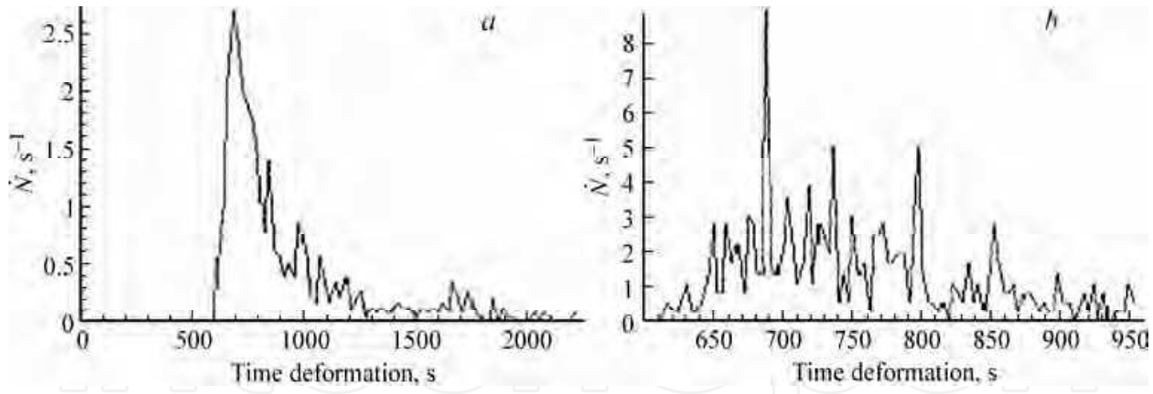

Fig. 23. AE activity Ṅ over all time of deformation of sample D16T – B(2.5%) (300° C) at deformation rate 0.118 mm/min (a), and the same in the time interval of multiple failures (650 to 950 s) (b).

In our opinion, the data given in figs 16-24 evidence unambiguously the dependence of possibility and "depth" of the development of the process of correlated cracking (fiber failures) on realization of the dissipative properties of material in the course of local stress redistribution. It is emerged that under particular conditions of experiment one can determine the dependence of the time delay of failure of fiber situated in the vicinity of fractured fiber on the amplitude of AE signal, which specifies the energy of elastic deformation released from broken fiber. Figure 25 shows such the dependence for the data depicted previously in fig. 22.

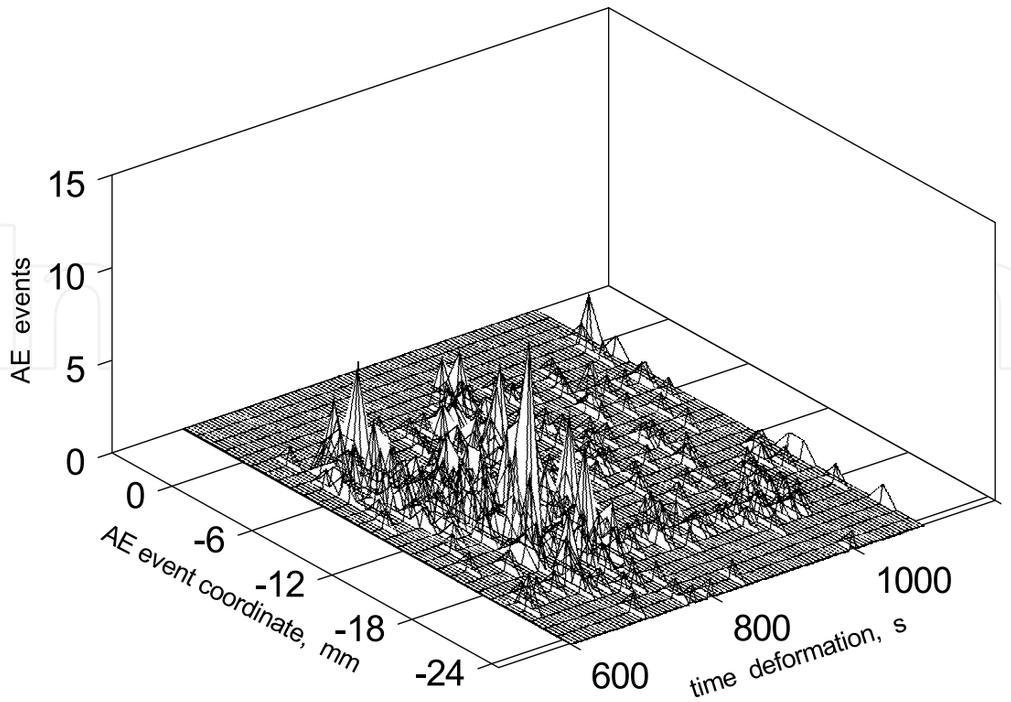

Fig. 24. 3D AE diagram of the fiber failure distribution in the course deforming of sample D16T – B(2,5 %) at deformation rate 0.118 mm/min and at elevated testing temperature 300^0 C.

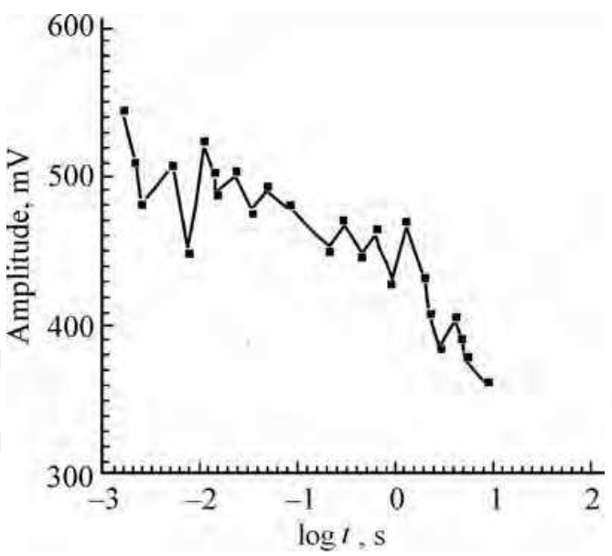

Fig. 25. Time delay of failure of fiber situated in vicinity of fractured fiber versus amplitude of AE signal.

This dependence (under the given conditions of the experiment) illustrates, in fact, the long-range influence of newly-forming defect on a similar neighboring structural element. It should be noted that this dependence is essentially a development of the results of experiments in situ (see fig. 2) for "structure-free" polymer with the help of the SEM technique as well as figures 3 and 4.

Surely, this result should be taken into account when constructing the physically grounded model of deformable heterogeneous solid.

When considering the general problem of emergence and evolution of the ensemble / cluster consisting of cracks of size close to that of structural elements, one should not overpass a very important aspect concerning the dissipative capability of solid as a whole. It was shown above that multiple starts of correlated crack nascence (each "attempt" could produce from a few unities to two tens of such cracks) are interlocked by a possibility to redirect this process to neighboring domains, which has conserved by the time their dissipative and deformation properties. In the simplest composites with a large volume content of high-strength and high-modulus fibers, the dissipative capabilities are, generally, sufficiently low.

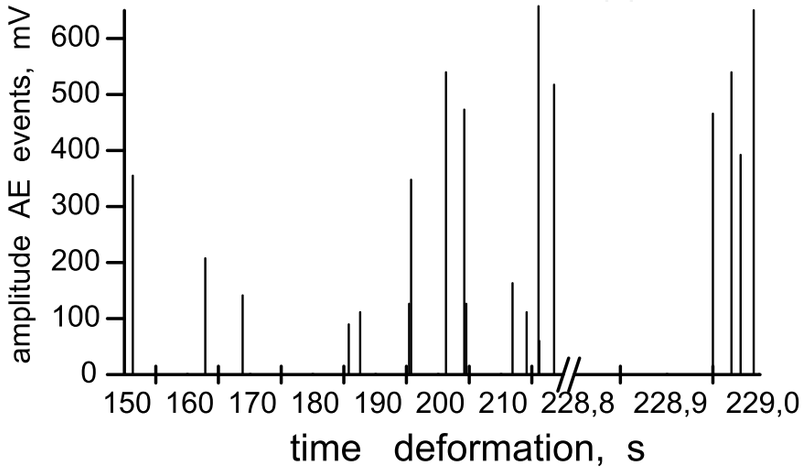

Fig. 26. Acoustic emission from the composite AMG61-B(43%) deformed at 0.118 mm/min, at 20°C.

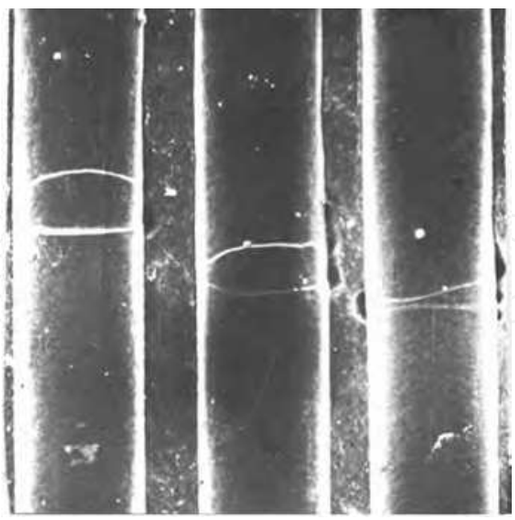

Fig. 27. Example of correlated failure of boron fibers in the sample with high volume content of fibers.

Figure 26 exhibits all the train of AE signals from the composite AMG61-B(43%) deformed at the rate 0.118 mm/min at 20°C. Total 21 signals were detected; 10 of them originated from

fiber failures (in accordance with the amplitude distribution depicted in fig. 14). Four final signals at 228.953 s, 228.967 s, 228.980 s and 228.994 s represent a sequence of correlated failures. The characteristic time of the stress increase at the fiber neighboring with the broken one is $\Delta t = 12 – 15$ ms.

Figure 27 shows an example of the correlated breakage of boron fibers of diameter of 100 μm.

5. Conclusion

To finalize, let us resume the results. The AE method in a mode of linear location was applied for studying the process of nucleation of cracks of size close to that of structural elements in composites deformed at constant rate. Two model unidirectional composites were used. The high-modulus composite was composed of carbon fibers (60 % by volume) embedded in polymer host, while the low-modulus one consisted of 1 to 2.5% of boron fibers embedded in the matrix based on aluminum alloy. Under conditions of combined deforming, a great difference in elastic modulus between the host and the reinforcing fibers provides the foremost failure of the high-modulus material and, correspondingly, the unequivocal identification of the sources of AE signals.

In the case of high-modulus composition, the multiple cracking at the initial stage of deforming runs as a poissonian-like process of independent, unconnected events, while at the last third of deformation cycle it runs as the process of correlated interaction. It is widely accepted that it is the last process leads to the formation of the main crack. Our experiment demonstrated another trend. As starting in a random domain, this process decelerates soon but, inevitably, a similar process becomes induced in a neighboring domain. A few attempts to organize the start of the main crack might occur.

When deforming a low-modulus composition, such as Al-B (2.5%), this trend is still more pronounced. Owing to the high energy release from failures of boron fibers, more significant long-range interactions take place, and the process of fiber failures manifests itself as the correlated process from the beginning of deforming.

However, multiple starts of the process of correlated crack nucleation (each “attempt” could produce from a few cracks to two tens of cracks) become obstructed by a possibility of redirecting of this process over adjacent domains, which, by that time, conserved still their dissipative, deformational capacities. The number of “false starts” as well as the length of a train of correlated failures might be governed by changing the conditions of running of dissipative processes. In the case of the composition containing a great amount of boron fibers (AMG61–B(43%)), such possibilities are, in fact, lacking. Therefore, the correlated failure of 3-4 fibers with time discontinuity of 12-15 milliseconds causes the macroscopic failure.

The performed experiments allows one to suggest that the higher the excess of energy absorption capability over the elastic strain energy released when a defect continuity nucleates, the greater number of meso/micro cracks might appear, and the interaction between them would be determined by the relaxation properties. Thereby, the stage of multiple crack formation is not critical à priori. The ensemble/ cluster of cracks is neither unavoidable nor necessary stage in the formation of the main crack. During the basic time of deforming, the discrete structural changes occur under conditions of sufficient dissipative

properties/ energy absorption capability. When this capacity becomes suppressed down to the critical level, a few explosion-like nucleation of mesocracks occurs as a result of emerging quasi-elastic interaction followed by the transition to the overcritical stage.

6. Acknowledgments

Author would like to thank A. Abdumanonov, G.N. Gubanova, A.P. Tishkin and V.E. Yudin for their assistance in performing model, acoustic emission measurements and useful discussion.

7. References

Arias, M. L., Frontini, P. M. & Williams, R.J.J. (2003) Analysis of the damage zone the crack tip for two rubber- modified epoxy matrices exhibiting different toughenability. Polymer. Vol. 44, p.p.1537-1546

Botvina, L. R.. (2008) *The destruction: kinetics*, mechanisms and *general laws*, Nauka, Moscow,2008 [in Russian]

Bouchbinder, E., David Kessler, D. & Procaccia, I. (2004) Crack-microcrack interactions in dynamical fracture. Phys. Rev. E 70, 046107

Braginski, A. P., Vinogradov, A. Yu. and Lekswskii (1986) *Acoustic amplitude*-frequency analysis of *the kinetics of deformation of metal glass.* Soviet Technical Physics Letters, Vol. 12, No. 9, p.p. 459-460

Kraus, R. Payer, A. & Wilke W. (1993) Acoustic emission analysis and small-angle X-ray scattering from microcracks during deformation of ETFE composites, J. of Materials Science, 28, p.p. 4047-4052

Leksowskij, A. M. and Baskin, B.L (2011) Some Aspects of Nucleation and Extension of Microskopic and Mesoscopic Cracks and Quasi-Brittle Fracture of Homogeneous Materials. Physics of the Solid State, Vol. 53, No, 6, p.p. 1223-1233

Leksowskij, A. M., Baskin, B.L, Tishkin, A.P. and Abdumanonov, A. A. (2008) Nonlinear Correlated Interaction of Mesodefects and Transition to Macrofracturing, Solid State Phenomena, Vol. 137, No.9, p.p. 9-14.

Nasseri, M., Mohanty, B. & Young, R. (2006) Fracture toughness measurements and acoustic emission activity in brittle rocks, Pure and Applied Geophysics, vol. 163, pp. 917-945,.

Regel', V. R., Slutsker, A. I., Tomashevskii, E. E. (1974) Kinetic Nature of Solids, Nauka, Moscow [in Russian]

Schors, J., Harbch., K.-W., Hentschel, M. and Lange., A. (2006) Non-Destructive Micro Crack Detection in Modern Materials, ECNDT - We.2.2.2

Tishkin,A. P., Gubanova, G. N., Leksowski, A. M. and Yudin, V. E. (1994) Acoustic emission data on delayed damage processes in the vicinity of defects fiber-reinforced plastics. J. of Materials Science, Vol. 29, p.p. 632-639

Tishkin, A. P. and Leksowski, A. M. (1988) *Correlation of the flow of acoustic emission events*. Soviet Technical Physics Letters, Vol. 14, No. 8, p.p. 636-638.

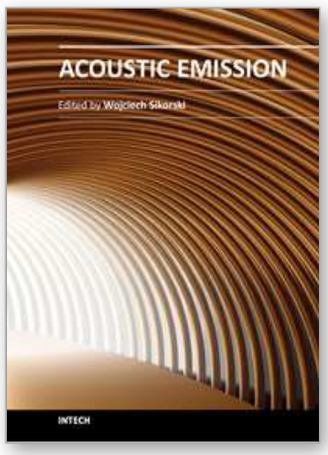

Acoustic Emission

Edited by Dr. Wojciech Sikorski

ISBN 978-953-51-0056-0
Hard cover, 398 pages
Publisher InTech
Published online 02, March, 2012
Published in print edition March, 2012

Acoustic emission (AE) is one of the most important non-destructive testing (NDT) methods for materials, constructions and machines. Acoustic emission is defined as the transient elastic energy that is spontaneously released when materials undergo deformation, fracture, or both. This interdisciplinary book consists of 17 chapters, which widely discuss the most important applications of AE method as machinery and civil structures condition assessment, fatigue and fracture materials research, detection of material defects and deformations, diagnostics of cutting tools and machine cutting process, monitoring of stress and ageing in materials, research, chemical reactions and phase transitions research, and earthquake prediction.

How to reference

In order to correctly reference this scholarly work, feel free to copy and paste the following:

Albert Leksovskii (2012). Delayed Fracturing: Acoustic Emission Analysis of Nucleation and Transformation of an Ensemble of Mesoscopic Cracks in Deforming Heterogeneous Materials, Acoustic Emission, Dr. Wojciech Sikorski (Ed.), ISBN: 978-953-51-0056-0, InTech, Available from: http://www.intechopen.com/books/acoustic-emission/delayed-fracturing-acoustic-emission-analysis-of-nucleation-and-transformation-of-an-ensemble-of-mes

INTECH
open science | open minds

InTech Europe
University Campus STeP Ri
Slavka Krautzeka 83/A
51000 Rijeka, Croatia
Phone: +385 (51) 770 447
Fax: +385 (51) 686 166
www.intechopen.com

InTech China
Unit 405, Office Block, Hotel Equatorial Shanghai
No.65, Yan An Road (West), Shanghai, 200040, China
中国上海市延安西路65号上海国际贵都大饭店办公楼405单元
Phone: +86-21-62489820
Fax: +86-21-62489821

IntechOpen